INFLUENCE OF THE NOZZLE GEOMETRY ON THE ATOMIZATION OF SUPERHEATED LIQUIDS

Markus Rossmeissl, Karl-Ernst Wirth

Department of Process Engineering, Institute of Particle Technology, University of Erlangen-Nuremberg
91058 Erlangen, Germany, sekretariat@lfg.uni-erlangen.de

ABSTRACT

Liquids are transferred into dispersions by different means of atomization. When using a plain-orifice nozzle a spray with very fine droplets of a few micrometers and small absolute velocities can be established by superheating liquids. The process of atomizing superheated liquids is one in which a liquid jet is disintegrated by the kinetic energy and the thermal energy of the partially evaporating liquid itself. Thus no make-up gases are necessary and the basic geometry of an orifice nozzle is applicable. The present paper reports about aspects of a work in progress. In particular the evaporation in the orifice nozzle is investigated experimentally. Nozzle geometry, pressure conditions and excess temperature are investigated in their influence on break-up characteristics of superheated ion exchanged water. Different spray characteristics, obtained by different length to diameter ratios of the investigated steel- and glass- nozzles, are based on high-speed-recordings, on mass-flow measurements on Particle-Image-Velocimetry and on Phase-Doppler-Analysis data. The observed phenomena can be referred to different flow pattern in the nozzle.

1 INTRODUCTION

Different mechanisms of atomizing liquids with certain energetic and process technological restrictions contribute to the formation of sprays. With respect to industrial throughputs, in rotary atomizers and vibration stimulated atomizers, moving parts have to be operated. In the field of plain-orifice atomizers and air-assist atomizers the quality of disintegration depends on the pressurization and on the volume throughput [3]. Above, with air-assist atomization the air-stream, which is necessary to disintegrate the liquid jet, is mixed with the generated liquid droplets in the spray and thus has to be extracted additionally as exhaust stream.

With the atomization of superheated liquids the benefits of a two-phase atomization and a pressure atomization can be combined. In this way disintegration with moderate pressure is superimposed to an effervescent atomization where steam bubbles evolve from nuclei and expand in the liquid stream. Consequently an internal-mixing steam-assist atomizer is obtained, in which the steam ratio depends on the operating point (pressure, temperature) and on the nozzle characteristics (geometry, material). By means of these parameters it is possible to obtain a spray with moderate droplet velocities.

With regard to subsequent applications of this technique in the chemical industry, it is aspired to produce either dry particles free of agglomerates respectively droplets with just one single particle. Thus a mode of operation has to be found, which leads to a narrow droplet size distribution of a few micrometers. Considering crystallisation processes in the vessel, the quench effect due to evaporation which cools down the droplets may be utilised for a simultaneous and selective stop of crystal growing. To this, low velocities in the spray are demanded, since an increased residence time of droplets lead to the option of applying a subsequent thermal process.

Previous works in the field of atomization of superheated suspensions were performed by Wellner/Wirth [1]. The task of this research was to understand the influence of particle properties on the characteristic of the spray cone. Thus the spray cone angle, the drop size distribution and the velocity field in the spray cone were investigated in their development with increasing excess temperature.

In the following the phenomenology of the atomization of superheated de-ionized water is presented according to a measurement matrix in which the degree of superheating (110°C-150°C), the pressure upstream the nozzle (1 - 7 bar), the length to diameter ratio of the nozzle orifice (7.7 – 28.5) as well as the material of the nozzle (steel, glass) were varied.

2 THEORETICAL BACKGROUND

2.1 Flash-Boiling

A liquid is defined as superheated if its temperature is above boiling temperature at present ambient pressure. Such a system is in the state of a thermodynamic non-equilibrium and thus unstable.

A stable thermodynamic equilibrium is obtained, if the superheated liquid is pressurized in a vessel to a pressure level above steam pressure of its respective temperature. When the system pressure is expanded to 1 bar ambient pressure, by means of an orifice nozzle at the bottom of the vessel, partial evaporation is occurring in the flowing liquid at locations where the pressure falls below steam pressure (flash-boiling). The occurrence of steam bubbles may already happen inside the nozzle. Outside the nozzle, it affects the sudden break up of the liquid jet and leads to the formation of ligaments and droplets. Above, the spray is in interaction with the ambient air, so that the momentum exchange with the air is of influence on the atomization of the liquid. The procedure of spray formation is supported by the reduction of viscosity and surface tension of the liquid with increasing temperature.

2.2 Relation of Liquid to Steam in the Spray

With the assumption that the steam and water fractions after the flash boiling have a temperature of 100°C, the respective mass- und volume fractions of steam can be derived from enthalpy considerations (having liquid phase h', ρ'; steam phase: h'', ρ''). According to Table 1 it becomes apparent that already at a small degree of superheating (110°C) a huge volume fraction of steam α is derived (96.8 vol.-%). Its rapid occurrence is the driving force for the break up of the water jet. Concerning the mass fraction x, the predominant fraction of the initially superheated liquid (> 98.1 mass-%) remains as liquid phase after the flash boiling.

Table 1: Characteristic numbers of the flash boiling of de-ionized water

temperature of the superheated water at the nozzle	ϑ	[°C]	110	130	150
steam pressure of water	p	[bar]	1.4	2.7	4.8
mass fraction of steam	x	[mass.-%]	1.9	5.5	9.2
volume fraction of steam	α	[vol.-%]	96.8	98.9	99.4

$$x = \frac{h'(\vartheta_0) - h'(\vartheta_1)}{h''(\vartheta_1) - h'(\vartheta_1)} \tag{1}$$

$$\alpha = \frac{x \cdot \rho'(\vartheta)}{x \cdot \rho'(\vartheta) + (1 - x) \cdot \rho''(\vartheta)} \tag{2}$$

2.3 Hydrodynamics of the Nozzle

Investigations to the atomization of liquid flows with formation of steam in orifice nozzles were carried out by Gebhard [2]. Depending on the pressure in the vessel upstream the nozzle different flow pattern may occur according to the l/d-ratio of the nozzle. As it will be discussed in chapter 4.1 three flow pattern in the capillary of the nozzle have to be distinguished.

By establishing a two-phase flow of water and air, Lörcher [3] investigated the context between the properties of the two phase mixture inside the nozzle and the properties of the resulting spray experimentally and as model. In the experimental part the gas-fraction was adjustable and thus accessible as parameter.

During the atomization process of superheated liquids the liquid is decompressed from the pressure level set at the nozzle to ambient pressure. During this procedure, steam pressure is passed through and the flow pattern in the nozzle as explained by Gebhart may occur. Since steam bubbles form in the liquid the effect of an inner mixing nozzle is derived, as it is described in the work of Lörcher. However, in contrast the steam fraction in the nozzle is not adjustable since it depends on the operating point (pressure in the vessel, excess temperature)

3 EXPERIMENTAL SET-UP AND MEASUREMENT TECHNIQUE

3.1 Experimental Set-up

The atomization of superheated liquids is carried out in a pilot plant, which is depicted in Figure 1.

A vessel storing and heating 25 litre de-ionised water to temperatures approaching 150°C is set under constant pressure. Constancy of temperature is achieved by a two-step-control of the wall heating while a stirrer ensures homogeneity of temperature. The static pressure in the vessel can be adjusted by a pressure controller up to 7 bar.

The orifice nozzle is mounted at the bottom of the vessel. As soon as the plug valve H6 is opened, the superheated water is transferred into the metastable state leading to an adiabatic expansion to ambient pressure and thus to the formation of a spray. In a vertical distance of 1 m to the nozzle, the spray is drawn off isokinetically by a fan.

The plant is run discontinuously. Since during experiments the facility is applied with constant pressure from the gas grid, a mass flow free of pulsation is ensured. Mass flow measurements are carried out by full-load measurements of the pressurized vessel within a time period of three minutes.

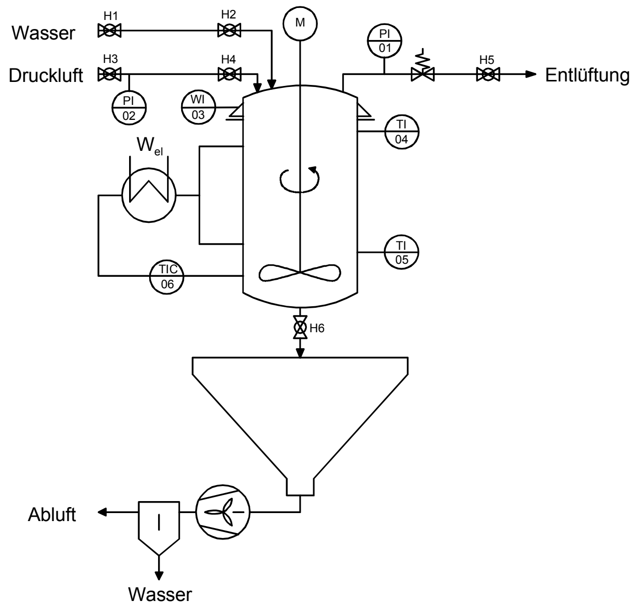

Figure 1: Flow chart for the atomization of superheated liquids

3.2 Orifice-Nozzles

Concerning the robust plain-orifice nozzle, focus was set on the hydrodynamics of the capillary flow in the nozzle. Thus on the one hand the ratio of length to diameter of the capillary and on the other hand the material of the nozzle was varied. Drilled steel nozzles with a diameter of bore of 0.9 mm as well as drawn glass nozzles with an internal diameter of 0.7 mm were used (see Figure 2). The lengths of these narrow capillaries were in each case 7 mm and 20 mm which lead to l/d-ratios of 7.7 and 22.2 for steel and 10.0 and 28.5 for glass.

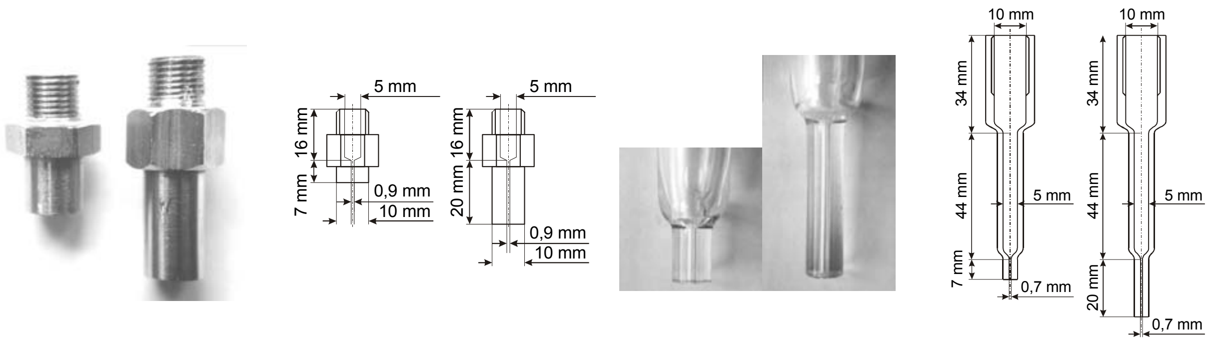

a) steel nozzle *b) glass nozzle*

Figure 2: Geometry of the nozzles

According to the applied pressure ranges of 1.4 to 7 bar in the vessel Reynolds numbers between 10^4 and 10^5 can be expected in the nozzle. Thus the flow in the cross section of the capillary of both, steel and glass nozzle, is turbulent [4].

3.3 Characterisation of the Spray

Different optical measurement techniques are applied in order to qualify the spray. By means of a high-speed-camera picture sequences of the flashing-process as it occurs at the outlet of the nozzles were captured. To this, the camera was operated with a long-distance-microscope and a flashlight system. With the aid of the Particle-Image-Velocimetry (PIV) the trajectory of droplets in the flow field within a laser-sheet plane was monitored and a global velocity field of the spray cone was recorded. Droplet velocities particularly of the vertical downward directed spray profile and corresponding droplet sizes were analysed by the Phase-Doppler-Anemometry (PDA)

4 RESULTS

4.1 Spray-Formation

Back-lighted pictures that were recorded with the high-speed-camera for both steel-nozzles at low degrees of superheating are presented in Figure 3. The near region was captured with five sequences of single pictures (5x5 mm each) that were arranged among one another. For every nozzle the development of the spray silhouette with increasing nozzle pressure drop, denoted as pressure difference Δp at a temperature of 110°C, is given.

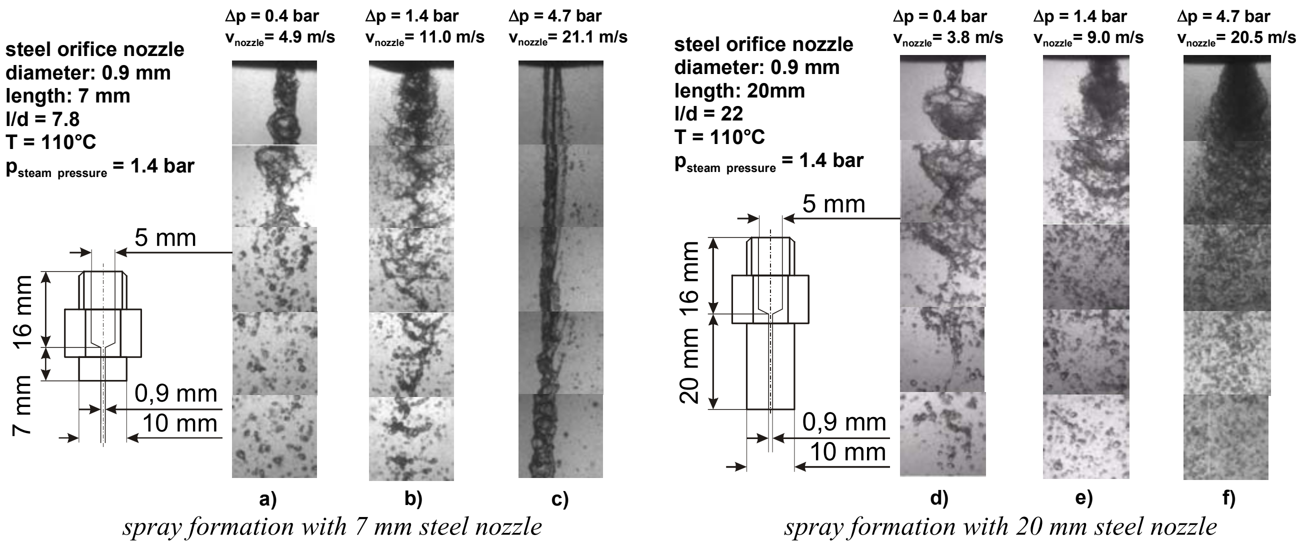

Figure 3: Disintegration in a superheated liquid at different nozzle geometries with increasing pressure at the nozzle.

A different l/d-ratio of the considered nozzles in Figure 3 leads to two different tendencies in disintegration with increasing pressure. While the initial formation of droplets and ligaments of the 7 mm steel nozzle is transformed into a continuous water jet with increasing pressure, the 20 mm steel nozzle shows an intensified degree of spray formation with fine droplets. Since both nozzles have the same sharp-edged inlet geometry (Figure 2), the observed spray pattern may be denoted to the different length of the nozzles.

According to the investigations of Gebhard [2] which are illustrated in Figure 4, three different flow-patterns can be distinguished for superheated fluids of constant velocities with respect to the l/d-ratio of the sharp-edged nozzle. Thus the superheated liquid initially forms an annular flow with steam at the wall, when being introduced into a plain orifice nozzle of l/d < 3. In this case a free flowing liquid jet can be expected. In the interval of 3 < l/d < 12, wherein the l/d-ratio of the given 7 mm nozzle is situated, first steam bubbles occur in the liquid and the two-phase flow tends to be no longer detached from the wall. The subsequent ejected multiphase flow may thus be still a pronounced water jet with sporadic droplet formations due to local flash-boiling. For longer nozzles of l/d > 12, which is given for the 20 mm steel nozzle, the liquid flow will finally be completely attached to the capillary wall and the density of steam bubbles in the liquid flow increases. The degree of local flash-boiling outside the nozzle increases and a fully developed spray may result.

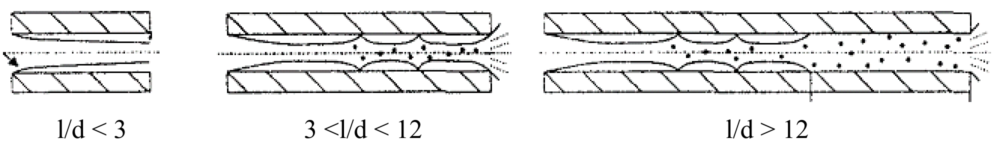

Figure 4: Flow pattern of a superheated liquid in a nozzle with different l/d-ratio at specific operation conditions.

Since the specific multiphase flow characteristics outside the nozzle that can be concluded from the research of Gebhard, for l/d-ratios of 3 <l/d < 12 in the 7 mm nozzle and l/d > 12 in the 20 mm nozzle can only be explicitly seen in the pictures c) and f) of Figure 3, a further influencing effect has to be considered. As Figure 3 displays, the development of the disintegrating water jet with increasing pressure difference shows a dependency on the flow velocity, i.e. a dependency of the residence time of the liquid in the nozzle. Above, the appearance of steam bubbles from forming nuclei is time-dependant. Thus the residence time of the liquid in the nozzle is a superimposed effect on the pure influence of the l/d-ratio. Due to this additional dependency, the spray picture that is derived for a given l/d ratio varies in terms of the varying pressure (flow velocity) that is applied, i.e. for low liquid velocities in the nozzle, the flow pattern of the spray for nozzles with 3 <l/d < 12 is shifted towards the flow pattern of nozzles with l/d > 12.

If the flow velocity will be increased in case of the 7 mm nozzle, the steam fraction in the nozzle will be reduced. The residence time in the nozzle is too short to form an adequate number of steam bubbles. Evaporation mainly occurs outside the nozzle at the surface of the water-jet, so that there is almost no jet break-up visible (Figure 3c)

In the 20 mm nozzle the adjacent flow leads to a longer residence time of the superheated liquid in the nozzle and thus to the formation of a higher number of growing bubbles. Therefore, the steam-fraction is bigger than in the 7 mm nozzle. With increasing flow velocity the quality of cross mixing enhances and a more homogeneous phase distribution in the nozzle results (Figure 3f).

Regarding the technical application of the process of atomizing superheated liquids, the degree of bubble formation respectively evaporation within the nozzle is relevant. On the one hand a homogeneously dispersed two-phase-flow from water and steam leads to a spray with fine droplets, while on the other hand a too big degree of evaporation in the nozzle brings about the risk of local dry out and thus of local blockages, in case of spraying superheated suspensions. However, long-term experiences about the atomization of suspensions in long nozzles are presently not at hand.

With back-lighted pictures it was shown that the break-up mechanism of the water jet is vitally influenced by evaporation processes in the nozzle. Evaporation may be prevented by smoother inlet geometries into the capillary of the nozzle. One possibility is the use of drawn glass nozzles. They stand for a low wall roughness and a steady reduction of the cross section. The development of the spray cone of investigated steel and glass nozzles with increasing excess temperature is summarized in Figure 5 by respective transmitted-light pictures of a CCD camera in the remote area.

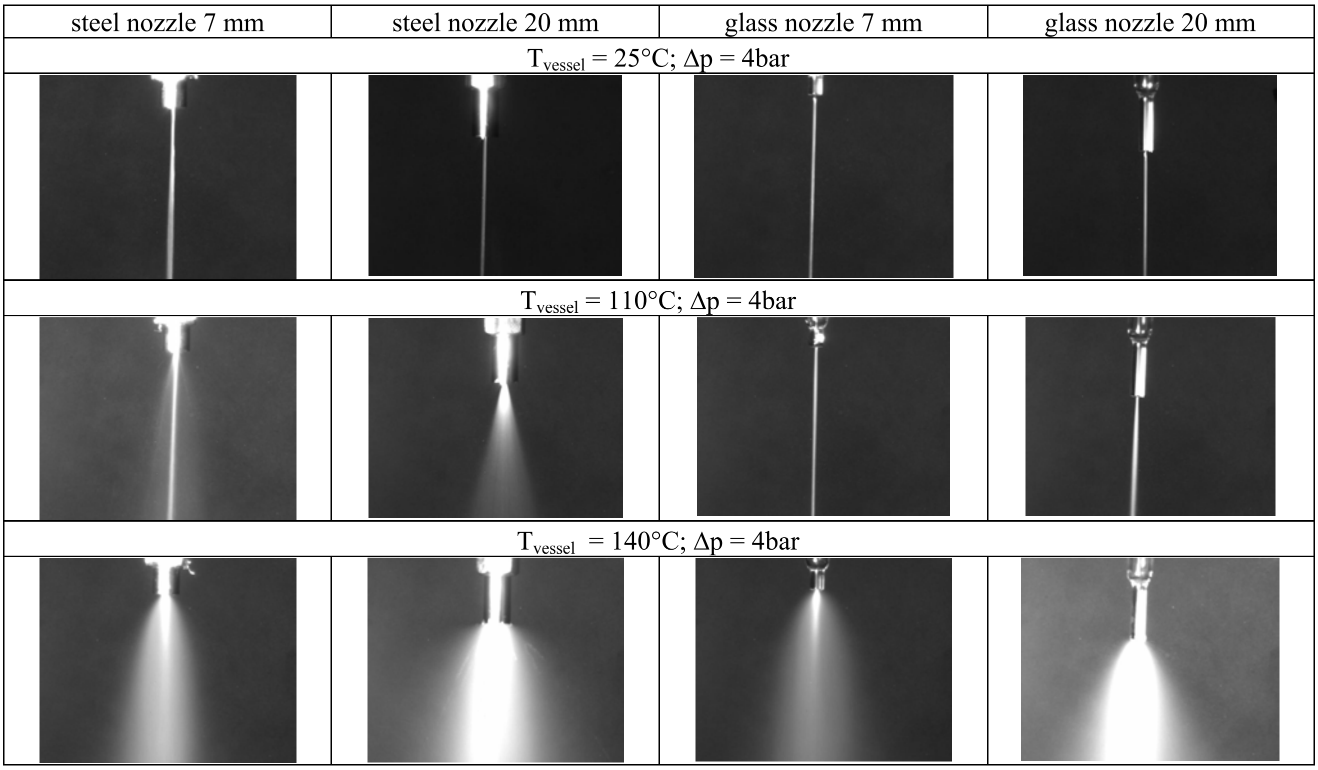

Figure 5: Spray silhouette of steel and glass nozzles with increasing degree of superheating

Figure 5 illustrates to which extend the degree of superheating affects the spray formation when using steel and glass nozzles at an operating pressure of 4 bar. For the pressurized atomization of water at temperatures of 25°C every nozzle exhibits a continuous undisturbed liquid jet along the vertical spray axis. When the water is superheated to 110°C, the glass nozzles still release a uniform water jet while it comes to a jet break-up for the steel nozzles. Thereby the disintegration of the 20 mm steel nozzle at 110°C appears homogeneous whereas there remains a dense liquid core for the 7 mm nozzle. Increasing the superheating to 140°C leads to disintegration also for the glass nozzles, particularly for the 20 mm long glass nozzle. Thus higher degrees of superheating, respectively diminishing the difference between pressure in the vessel (4 bar) and the temperature depending steam pressure, provokes the formation of bubble nuclei at the wall of the nozzle and partial evaporation occurs in the nozzle. At such operation conditions glass nozzles behave just as steel nozzles.

With the application of the material glass, the evaporation that initially starts in the steel nozzle at low degrees of superheating can be predominantly shifted outside the nozzle. At 110°C no break-up can be noticed for the glass nozzle so that evaporation sets in from the jet surface. Contrarily to this, an initial formation of steam bubbles in the steel nozzle can be assumed which initiates the disintegration already for 110°C.

Visual watching through the 20 mm glass nozzle showed how a fortuitous point defect in the 20 mm capillary could activate a sudden evaporation. From this point the flow in the capillary was opaque while in another 20 mm glass nozzle the flow was continuously transparent.

4.2 Break-Up of the Water Jet

To classify the break-up mechanism active for the disintegration of superheated liquids with orifice nozzles, the obtained data where inserted into the Ohnesorge diagram. The Ohnesorge-number (Oh) combines material constants of the fluid-system, as the surface tension $\sigma_f(T)$, the liquid density $\rho_f(T)$ and the dynamic viscosity $\eta_f(T)$, which characterise the disintegration. The Oh-number results from the ratio between Weber-number (We; ratio of momentum and surface forces) and the Reynolds-number (Re; ratio of inertia and viscous forces) and refers to the outlet diameter d of the respective nozzle. The Reynolds-number is fed with the velocity of the superheated liquid in the nozzle v_{nozzle}, which is derived by mass-flow-measurements. Thus in the Ohnesorge-diagram the degree of superheating is solely accounted for with the temperature dependence of the fluid constants

$$\mathrm{Oh} = \frac{\sqrt{\mathrm{We}}}{\mathrm{Re}} = \frac{\eta_f}{\sqrt{\rho_f \cdot \sigma_f \cdot d}}; \qquad \mathrm{Re} = \frac{\rho_f \cdot v_{nozzle} \cdot d}{\eta_f} \tag{3}$$

Pursuant the Ohnesorge-diagram, depicted in Figure 6, in which an increment of the pressure in the vessel leads to an increased liquid velocity and thus a horizontal translation of the operation point, the break-up of the water jet can be attributed to the transition area from wave break-up to atomization. Subsequent effects of an effervescent nozzle, of aerodynamical interactions with the ambient air and continuing evaporation finally lead to the disintegration of the superheated liquid. This progress can already be seen in Figure 5, where the disintegration does not start until the liquid is superheated. A sole pressurized atomization at 4 bar does not exist.

As a result of the momentum exchange with the ambient atmosphere different velocity profiles of liquid droplets in the spray cone evolve according to the examined nozzle types. The velocity profile of the 7 mm glass and steel nozzle derived by Particle Image Velocimetry is presented in Figure 7.

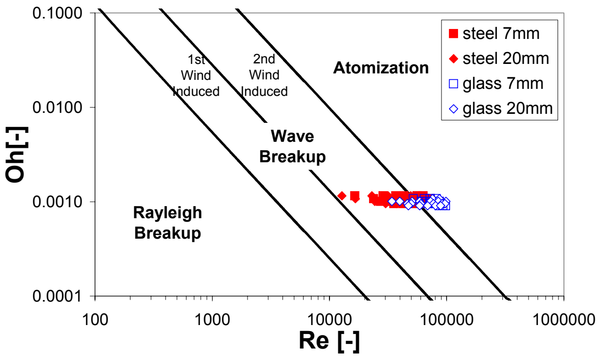

Figure 6: Break-up regimes in the chart of Ohnesorge according to Reitz [5]

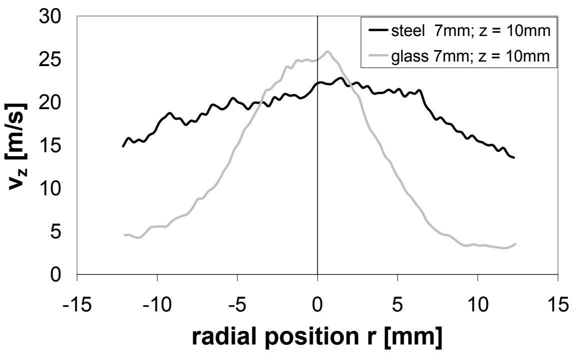

Figure 7: Velocity profile in the spray cone in 10 mm vertical distance to the nozzle T_{vessel} = 140°C; Δp = 4bar; PIV-measurement

In comparison to the wider spray cone angle of the 7 mm steel nozzle, depicted in Figure 5, the velocity profile of the 7 mm glass nozzle shows steeper gradients, while even having a continuous dense core. For the curves in Figure 7 date were captured for radial positions of up to r = ± 12.5 mm, because for larger radii only a few particles could be detected and thus no statistically verified velocity data are present. This maximum radius up to which data acquisition was carried out, will consequently be denoted as R.

4.3 Mass Flow Measurements

In order to acquire the flow rate of the superheated medium through the orifice nozzles, mass-flow-measurements have been carried out. They give information about which degree of dispersion out of steam and liquid phase is present. At first the mass flow obtained for the steel nozzles was plotted versus the pressure in the vessel in Figure 8a. Since the diameter of the orifice of the glass and the steel nozzles are different (see Figure 2) a comparison between both materials was carried out in Figure 8b by relating the mass flow to the outlet cross-section. Hence the mass-flow density is derived.

From Figure 8a it arises to what extend the l/d-ratio has influence on the hydrodynamics in the examined steel nozzles. The highest mass flows were measured for temperatures of 35°C. At this temperature where no jet break-up occurs, the mass flow is independent from the l/d ratio, since both curves course almost congruently. In the case of the liquid at excess temperature the mass flow decreases with increasing superheating. The mass flow curves of the 20 mm steel nozzle run below the corresponding curve of the 7 mm steel nozzle. The increased momentum exchange between steam and liquid phase obviously leads to an increased pressure drop in the nozzle capillary. In consequence the mass flow reduces with rising l/d-ratio. Indications that the critical mass flow is already reached for the flow of superheated liquid through the nozzle within the applied pressure range from ambient to 7 bar are given. However they still have to be proven with a setup that gives the opportunity to increase the pressure of the ambience into which the spray is released.

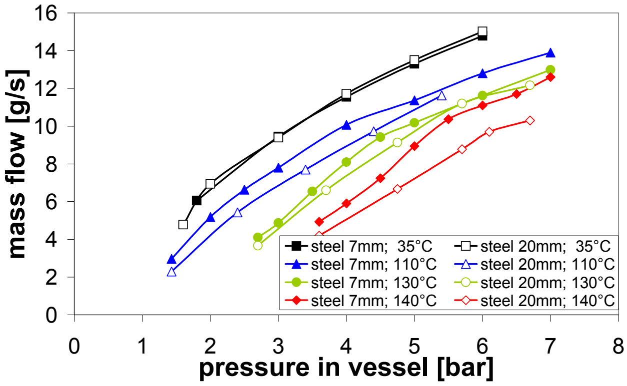

a) Mass-flow-density of the steel nozzle

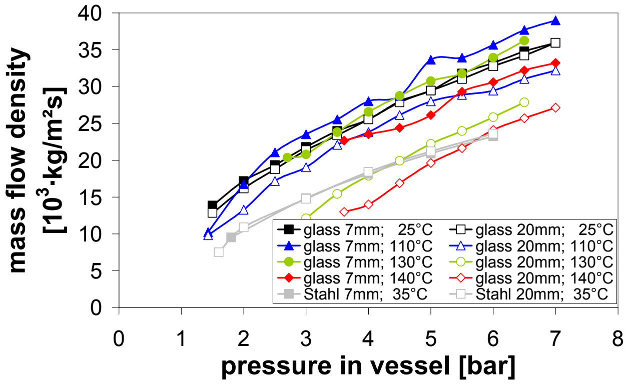

b) Mass-flow-density of the glass-nozzle in comparison to the steel nozzle

Figure 8: Mass flow resp. mass flow density with increasing degree of superheating and rising pressure in the vessel

In the comparison between glass and steel nozzles in Figure 8, each mass flow density of glass nozzles is located above those of the steel nozzle at equal temperature, when regarding the maximum mass flow curve of the steel nozzle at 35°C as reference curve. The continuously reducing inlet geometry of the capillary and the lower surface roughness of the inner wall can be considered as main reasons for the lower pressure drop in the glass nozzles. Just as with the steel nozzles, also the glass nozzles prove that their mass flow at ambient temperature is independent from the l/d-ratio. A decreasing mass flow with applied superheating can be observed from temperatures above 130°C. This result can be referred to observations about the spray evolution with increasing pressure at the nozzle, which were published in Figure 5. Herein the evaporation and thus the atomization process for the glass nozzles start at temperatures between 110°C and 140°C.

Due to the reduced viscosity, the mass flow density of the slightly superheated liquid in the 7 mm glass nozzle is even above those at ambient temperature. This can be seen as further indication that there is no multiphase flow in the glass nozzle for low superheating temperatures.

The energy of the system provided by pressurizing and superheating the liquid is transferred by the plain orifice nozzles into kinetic energy, into dissipation and into energy for the formation of new liquid surfaces. The degree of surface formation in the spray is measured by droplet size distributions with Phase Doppler Anemometry (PDA). To this a radial profile of droplet sizes was captured in two horizontal planes (5 cm und 10 cm) below the nozzle, which is plotted as $d_{50,0}$-values within a cumulative number distribution curve in Figure 9. The operational settings for obtaining the $d_{50,0}$-values were the same in all spray cones

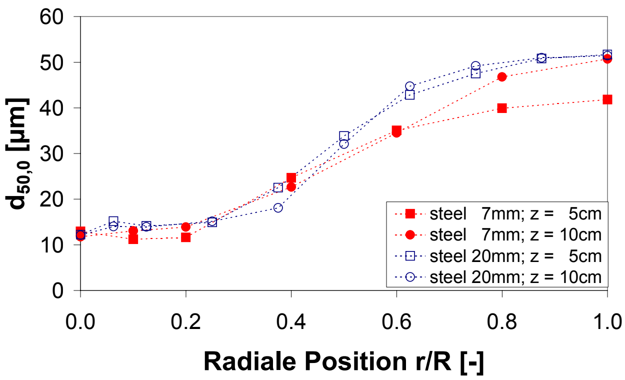

a) $d_{50,0}$-values of the steel nozzles

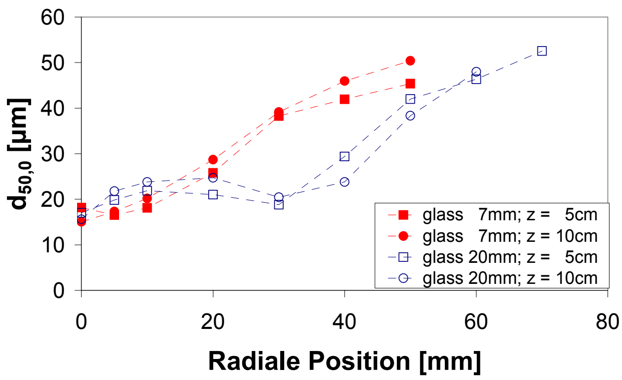

b) $d_{50,0}$-values of the glass nozzles

Figure 9: Development of the mean drop-size ($d_{50,0}$-value) in the spray cone on two planes in 5 cm and 10 cm distance to the nozzle; T_{vessel} = 140°C; Δp = 6 bar

From the $d_{50,0}$-values in Figure 9 it becomes apparent for both, steel- (a) and glass-nozzles (b) that the mean droplet diameter grows with increasing radial distance to the vertical spray axis. According to this, the fraction of fine droplets is higher in the core than in the annulus of the spray. A qualitative estimation of the mass flow distribution of liquid over the cross section of the spray cone, which was derived from PDA data, points up that 95% of the total liquid mass flow is distributed within the spray core of r/R = 0.5 and thus over just 25% of the total spray cross section (Figure 10).

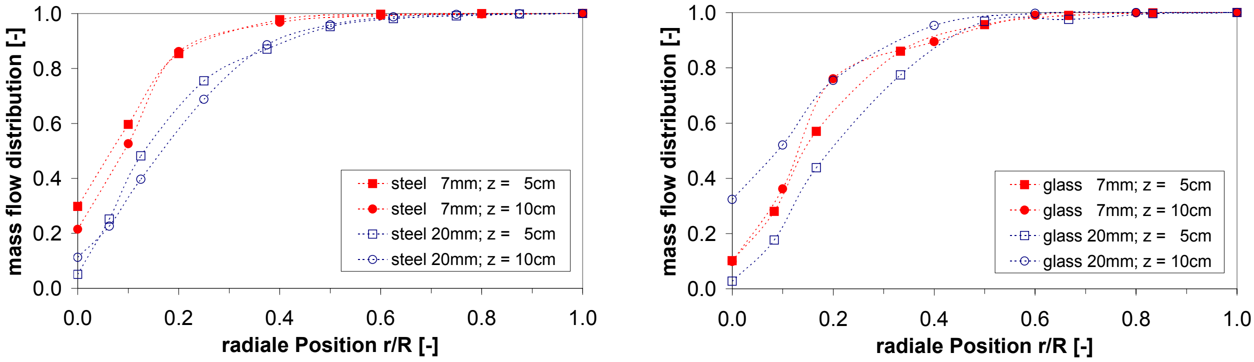

a) steel nozzle *b) glass nozzle*

Figure 10: Distribution of the liquid fraction in the spray on two planes in 5 cm and 10 cm distance to the nozzle

Based on the absolute radial position, the drop sizes of the 7 mm nozzle are bigger than those of the 20 mm nozzle. This was already denoted in Figure 5 where a larger spray cone angle for the 20 mm nozzles (steel and glass) could be recognized in comparison to the 7 mm nozzles. Thus the radial acceleration after ejection holds the higher potential to form new liquid surfaces. Consequently the amount of energy that is transferred into new liquid surfaces is higher for 20 mm nozzles than for 7 mm nozzles and it is accordingly higher for steel nozzles rather than for glass nozzles.

5 SUMMARY

To characterize the jet break-up of supercritical water, mass flow measurements, optical and laser-optical observations were carried out in the near field region of plain orifice nozzles. By investigating steel and glass nozzles of analogue l/d-ratios, the behaviour of a quasi-inner mixing nozzle that occurs due to partially evaporation within the nozzle could be checked.

While the increment of the l/d-ratio in drilled steel nozzles lead to increased amount of steam in the nozzle orifice and thus to a finer spray, the thermodynamically same quality of evaporation at glass nozzles could be predominantly shifted outside the orifice. Thus, with the aid of glass nozzles, the evaporation that is basically captured in the capillary of the steel nozzle is experimentally accessible.

With respect to the drop size distribution within the spray cone, two main areas could be distinguished. While in the core area of the spray ($r/R < 0.5$) mean droplet diameters of 10 to 25 µm were measured, the drop size in the annulus area was 50 µm. An estimation of the mass flow distribution of the liquid over the cross section resulted in the awareness that 95% of the total mass of the liquid is present as fine droplets of 10-20 µm and is captured within 25% of the inner area of the spray core. Contrarily big droplets of 20-50 µm that stand for 5% of the total liquid can be found in the annulus area of the spray cone (75% cross sectional area). The mechanism behind the presence of a bimodal drop size distribution within the spray cone still has to be investigated.

6 ACKNOWLEDGEMENTS

The financial support by the German Research Foundation (DFG) is gratefully acknowledged.

7 NOMENCLATURE

d	nozzle diameter	[m]	T	temperature	[K]
$d_{50,0}$	mean droplet diameter	[µm]	v	velocity	[m/s]
h	enthalpy	[kJ/kg]	We	Weber number	[-]
l	nozzle length	[m]	x	mass fraction of steam	[mass-%]
Oh	Ohnesorge number	[-]	z	vertical distance	[m]
p	pressure	[bar]			
r	radial position	[m]	α	volume fraction of steam	[vol-%]
R	maximum radius	[m]	η	dynamic viscosity	[kg/m s]
Re	Reynolds number	[-]	ϑ	temperature	[°C]

8 REFERENCES

1. Wellner S., Wirth K.-E.: Atomization of superheated suspensions with different solids and solid concentrations, ILASS-Europe 2001, Zurich, 2001.
2. Gebhard P.: Zerfall und Verdampfung von Einspritzstrahlen aus lamellenbildenden Düsen, Ph.D. thesis, Technische Universität München, pp. 23-25, 1996.
3. Lörcher M.: Zerstäuben von zweiphasigen Gemischen aus Flüssigkeiten und Gasen, Fortschrittberichte VDI, Reihe 3, Nr. 764, 2002.
4. VDI-Wärmeatlas: Druckverlust bei der Durchströmung von Rohren, Lb2, 6. Auflage, 1991.
5. Reitz R.D., Bracco F.V.: Ultra-High-Speed Filming of Atomizing Jets, Phys. Fluids 22, pp. 1054-1064, 1979.